LAWRENCE
LIVERMORE
NATIONAL
LABORATORY

LLNL-CONF-679408

Cold Nuclear Matter Effects on J/psi and Upsilon production in p+Pb collisions at 5 TeV and Pb+Pb collisions at 5.1 TeV

R. Vogt

November 17, 2015

Quark Matter 2015
Kobe, Japan
September 28, 2015 through October 3, 2015

Disclaimer

This document was prepared as an account of work sponsored by an agency of the United States government. Neither the United States government nor Lawrence Livermore National Security, LLC, nor any of their employees makes any warranty, expressed or implied, or assumes any legal liability or responsibility for the accuracy, completeness, or usefulness of any information, apparatus, product, or process disclosed, or represents that its use would not infringe privately owned rights. Reference herein to any specific commercial product, process, or service by trade name, trademark, manufacturer, or otherwise does not necessarily constitute or imply its endorsement, recommendation, or favoring by the United States government or Lawrence Livermore National Security, LLC. The views and opinions of authors expressed herein do not necessarily state or reflect those of the United States government or Lawrence Livermore National Security, LLC, and shall not be used for advertising or product endorsement purposes.

Available online at www.sciencedirect.com
ScienceDirect
Nuclear Physics A 00 (2015) 1–4
Nuclear Physics A
www.elsevier.com/locate/procedia

Cold Nuclear Matter Effects on J/ψ and Υ production in p+Pb collisions at 5 TeV and Pb+Pb collisions at 5.1 TeV

R. Vogt

Nuclear and Chemical Sciences Division, Lawrence Livermore National Laboratory, Livermore, CA 94551, USA
Physics Department, University of California, Davis, CA 95616, USA

Abstract

We make a systematic study of the modifications of J/ψ and $\Upsilon(1S)$ production in p+Pb collisions at $\sqrt{s_{NN}}$ = 5 TeV at the LHC. We compare the uncertainties in the EPS09 shadowing parameterization to the calculated mass and scale uncertainties obtained employng the EPS09 NLO central set. We study the dependence of the results on the proton parton density and the choice of the nuclear modifications. We check whether the results obtained are consistent at leading and next-to-leading order. The calculations are compared to the available ALICE and LHCb data on the nuclear modification factors, $R_{pA}(y)$ and $R_{pA}(p_T)$, as well as the forward-backward asymmetries, $R_{FB}(y)$ and $R_{FB}(p_T)$. Finally, we make predictions for the next Pb+Pb run at $\sqrt{s_{NN}}$ = 5.1 TeV in Run 2 of the LHC.

Keywords:

1. Introduction

Proton-nucleus collisions have been used as a intermediate baseline for the determination of cold medium effects. They lie between proton-proton collisions in vacuum and nucleus-nucleus collisions which are expected to be dominated by hot matter effects. Modifications of the quark densities in nuclei relative to those of the proton are well established although those of the gluons in the nucleus are not well understood. We focus on the effect of these on quarkonium production in proton-lead collisions at the LHC at a center of mass energy of 5.02 TeV. We determine whether it is possible for the LHC proton-lead data to be described by nuclear modifications of the parton densities, referred to as shadowing, alone.

Here we show a selection of results from Ref. [1]. We employ the color evaporation model of quarkonium production at next-to-leading order in the total cross section and leading order in the transverse momentum dependence. We study the choice of shadowing parameterization on the result. We also investigate the size of the mass and scale uncertainties relative to the uncertainty on the shadowing parameterization, both on the cross section and the ratio of cross sections. Finally, we show predictions for the p_T dependence of the Pb+Pb results at $\sqrt{s}$ = 5.1 TeV for the EPS09 NLO [2] shadowing parameterization. For the full results, including R_{FB}, $R_{p\mathrm{Pb}}(y)$ and the p_T dependence of $R_{p\mathrm{Pb}}$ at backward and midrapidity, as well as all the Υ results, see Ref. [1].

2. Results

We use the same values of the charm quark mass and scale parameters as found in Ref. [3] to obtain the normalization F_C for the J/ψ, $(m, \mu_F/m, \mu_R/m) = (1.27 \pm 0.09\,\text{GeV}, 2.1^{+2.55}_{-0.85}, 1.6^{+0.11}_{-0.12})$. In the case of Υ production, we employ $(m, \mu_F/m, \mu_R/m) = (4.65 \pm 0.09\,\text{GeV}, 1.4^{+0.77}_{-0.49}, 1.1^{+0.22}_{-0.20})$. The calculations shown here employ the CT10 proton parton densities [4]. We determine F_C only for the central parameter set in each case and scale all the other calculations by the same value of F_C to obtain the extent of the J/ψ and Υ mass and scale uncertainty bands. We compare our results to the ALICE J/ψ data [5, 6] here.

Figure 1 compares the suppression factors for $J/\psi \to \mu^+\mu^-$ at forward and backward rapidity as a function of p_T calculated with different nuclear modifications of the parton densities (nPDFs). the spread between predictions is largest in the forward region where the shadowing predictions differ most. Indeed, in the p_T bin centered at 1.5 GeV, there is a factor of ~ 8 between the values of $R_{p\text{Pb}}$. The gap is reduced to ~ 1.3 by $p_T \sim 3.5$ GeV. The weakest p_T dependence is given by the calculations with nDS [8] and the central EPS09 NLO set [2]. The nDSg [8] set also results in a weak p_T dependence but has a stronger overall shadowing effect. The strongest shadowing comes from the FGS sets [7] which overpredict the shadowing strength. The best agreement with the data is obtained for the EKS98 LO set [9, 10] which has no NLO counterpart. Note that the measured $R_{p\text{Pb}}$ approaches unity at $p_T \sim 7$ GeV while none of the shadowing parameterizations give a result approaching unity over the entire p_T range shown. In the backward region the results show antishadowing except for nDS and nDSg which specifically exclude it. All the calculations lie below the centroids of the data, partly because the ALICE acceptance is centered on the side of the antishadowing peak so that the calculated antishadowing is, on average, lower than that of the data. Note also that the antishadowing peak is broad in p_T, with some antishadowing remaining at $p_T \sim 15$ GeV.

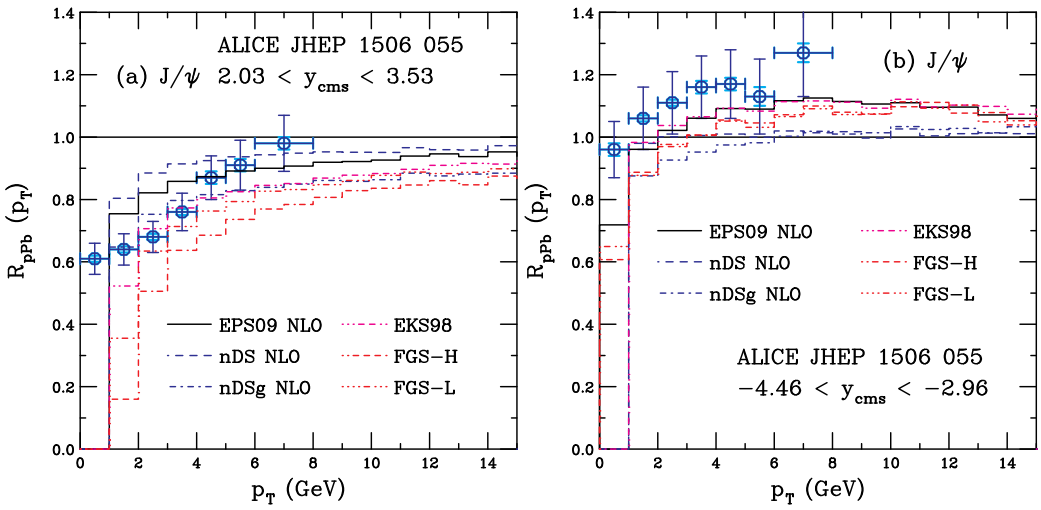

Fig. 1. (Color online) The J/ψ ratio $R_{p\text{Pb}}(p_T)$ in the ALICE acceptance at forward (a) and backward (b) rapidity [6]. The results are shown for central EPS09 NLO [2] (black), nDS NLO (blue dashed) [8], nDSg NLO (blue dot-dashed) [8], EKS98 LO (magenta dot-dot-dash-dashed) [9, 10], FGS-H (red dot-dash-dash-dashed) [7] and FGS-L (red dot-dot-dot-dash) [7].

We now turn to the mass and scale uncertainties of the results, calculated based on the one standard deviation uncertainties on the quark mass and scale parameters [3]. If the central, upper and lower limits of $\mu_{R,F}/m$ are denoted as C, H, and L respectively, then the seven sets corresponding to the scale uncertainty are $\{(\mu_F/m, \mu_F/m)\} = \{(C,C), (H,H), (L,L), (C,L), (L,C), (C,H), (H,C)\}$. The uncertainty band can be obtained for the best fit sets by adding the uncertainties from the mass and scale variations in quadrature. The uncertainties of the EPS09 NLO nPDF sets compared to those of the mass and scale for $d\sigma/dp_T$ at forward rapidity are shown in Fig. 2(a) for the J/ψ, based on the EPS09 NLO central set. The red solid and dashed curves are the central EPS09 NLO results with the uncertainty band due to the EPS09 parameter

variations. The magenta curves in Fig. 2(a) show the uncertainty due to the mass and scale variations. The lowest p_T results are not shown because the underlying $p + p$ calculation does not accurately numerically cancel the divergences in the negative weight Monte Carlo [11]. The intrinsic k_T kick used to obtain the shape of the p_T distribution in the low-p_T region was fixed at RHIC energies and successfully compared to the J/ψ p_T distributions at $\sqrt{s}$ = 7 TeV [3].

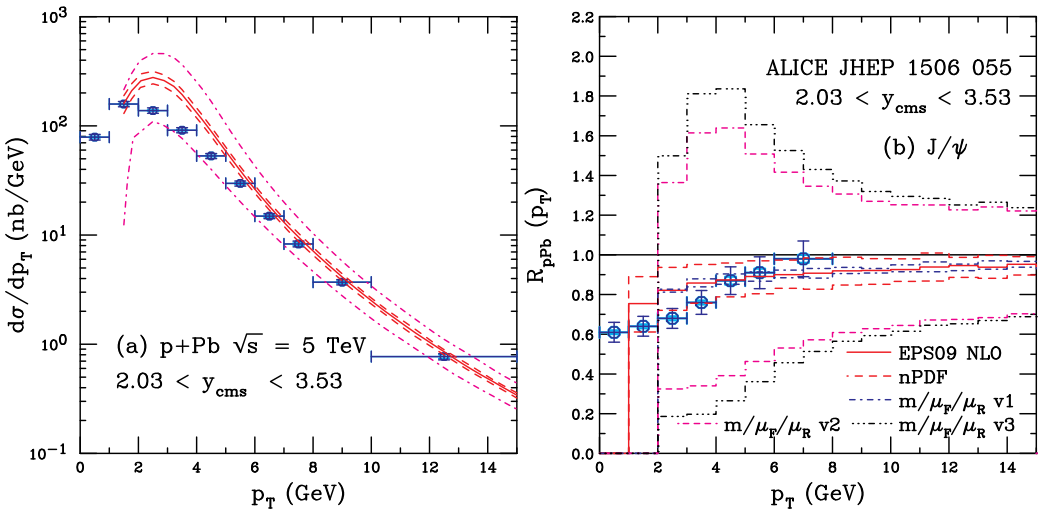

Fig. 2. (Color online) (a) The ALICE J/ψ p_T distributions [6] at forward rapidity at NLO in the CEM [3]. The solid red curve is the EPS09 NLO central value while the dashed red curves are the EPS09 NLO uncertainties and the dot-dashed magenta curves are the mass and scale uncertainties. (b) The mass and scale uncertainties in the J/ψ ratio $R_{p\mathrm{Pb}}(p_T)$ at forward rapidity [6]. The EPS09 NLO uncertainty band is shown in by the red dashed curves while the uncertainties calculated with method $v1$ are shown in the blue dot-dashed curves; $v2$ in the magenta dot-dash-dash-dashed curves; and $v3$ in the black dot-dot-dot-dashed curves.

The mass and scale dependence of $R_{p\mathrm{Pb}}(p_T)$ depends on whether the uncertainty band is formed by taking the ratios of p+Pb to $p + p$ for each mass and scale set, which is essentially the uncertainty of the EPS09 central set, $v1$, or forming the mass and scale uncertainty band for p+Pb based on the cross sections and then taking ratio to the central $p + p$ cross section, $v2$. Here $v2$ is comparable to the procedure for calculating the uncertainty band on a given distribution, such as $d\sigma/dp_T$, while $v1$ would tend underestimate the cross section uncertainty and even lead to an uncertainty smaller than that of the shadowing parameterization itself. These are both calculated adding the extrema in the mass and scale variations in quadrature, as in Refs. [1, 12]. Another method, $v3$, calculates the scale uncertainties in quadrature for $(\mu_F/mu, \mu_R/m)$ pairs $[(H, H), (L, L)]$, $[(H, C), (L, C)]$ and $[(C, H), (C, L)]$ instead of only using extrema. (There is only one mass pair.) These results are very similar to v_2 albeit giving somewhat larger uncertainties.

Figure 2(b) shows the relative uncertainties for the EPS09 NLO band and the three ways of calculating the mass and scale uncertainty for $R_{p\mathrm{Pb}}(p_T)$ at forward rapidity. As expected, $v1$ gives the smallest uncertainty since there is little variation in the individual values of $R_{p\mathrm{Pb}}$ for each mass and scale choice for the central EPS09 set. Therefore, the $v1$ band is narrower than that of the EPS09 band itself, underestimating the uncertainty. The $v2$ and $v3$ bands are wider, especially for $p_T < 5$ GeV, as expected. The $v3$ band is broader than that of $v2$ over all p_T although the two methods merge at the highest p_T values. The $R_{p\mathrm{Pb}}(p_T)$ found for the $v2$ method is in agreement with what one might expect looking at the bands on $d\sigma/dp_T$ in Fig. 2(a).

The predicted p_T dependence of the nuclear modification factor in Pb+Pb collisions, R_{PbPb}, is shown for both J/ψ and Υ production at $\sqrt{s}$ = 5.1 TeV in the forward region, $2.5 < y < 4$, in Fig. 3. In this symmetric system, there is no rapidity shift. There is shadowing at low p_T on the J/ψ with antishadowing at $p_T > 10$ GeV. The ratio becomes equivalent to unity at higher p_T. For the Υ, shadowing effects are small and the uncertainty band gives a result equivalent to unity over all p_T in this y range. The result is a convolution

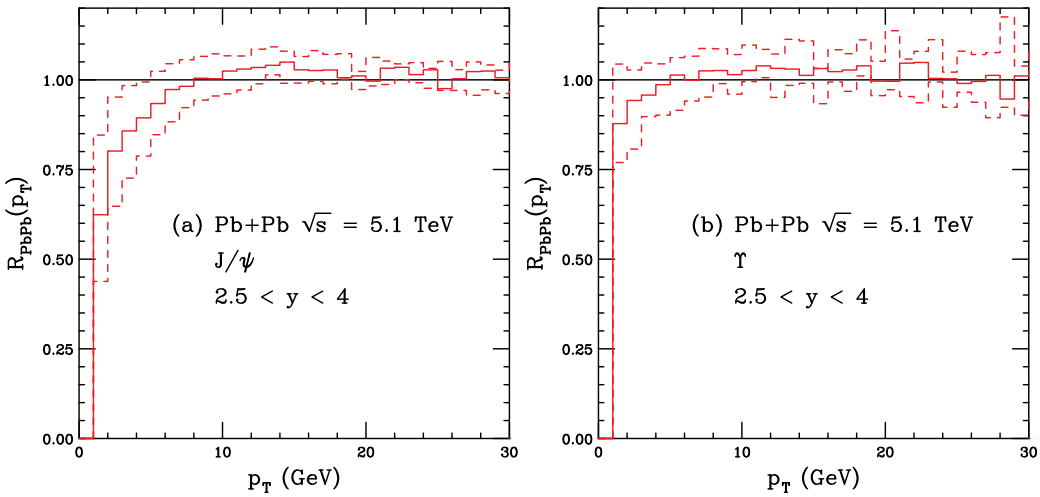

Fig. 3. (Color online) The EPS09 NLO uncertainty band as a function of p_T at forward rapidity for J/ψ (a) and Υ (b) in Pb+Pb collisions at $\sqrt{s}$ = 5.1 TeV.

of the p+Pb ratios, $R_{p\mathrm{Pb}}(p_T; 2.5 < y < 4)$, in the shadowing region, and $R_{p\mathrm{Pb}}(p_T; -4 < y < -2.5)$, in the antishadowing region. Since the p+Pb data were taken at $\sqrt{s}$ = 5.02 TeV, these data can be use to obtain the cold nuclear matter expectation for ground state quarkonium production in these collisions.

3. Conclusions

The rapidity and p_T dependence of the nuclear modification factor, $R_{p\mathrm{Pb}}$, are generally consistent with the next-to-leading order calculations in the color evaporation model, including shadowing, within the uncertainties. However, the forward-backward ratio is more difficult to describe with shadowing alone [1], except for calculations with the LO EKS98 set, employed in a NLO calculation. Data from $p + p$ collisions at the same energy are needed. The mass and scale uncertainties on $R_{p\mathrm{Pb}}$ are larger than those of the nuclear parton densities. Predictions for the shadowing effects in Pb+Pb collisions at $\sqrt{s}$ = 5.1 TeV, shown here, can be approximately obtained from convolutions of the p+Pb collisions at $\sqrt{s}$ = 5 TeV.

The improved d+Au data from RHIC and the p+Pb data from the LHC suggest that it is time for a new global analysis of the nuclear modifications of the parton densities, taking the new data into account.

Prepared by LLNL under Contract DE-AC52-07NA27344.

References

[1] R. Vogt, arXiv:1507.04418 [hep-ph].
[2] K. J. Eskola, H. Paukkunen and C. A. Salgado, JHEP **0904**, 065 (2009).
[3] R. E. Nelson, R. Vogt and A. D. Frawley, Phys. Rev. C **87** (2013) 014908.
[4] H. L. Lai, M. Guzzi, J. Huston, Z. Li, P. Nadolsky, J. Pumplin, C.-P. Yuan, Phys. Rev. D **82**, 074024 (2010).
[5] B. Abelev *et al.* (ALICE Collaboration), JHEP **1402**, 073 (2014).
[6] J. Adam *et al.* (ALICE Collaboration), JHEP **1506**, 055 (2015).
[7] L. Frankfurt, V. Guzey and M. Strikman, Phys. Rept. **512**, 255 (2012).
[8] D. de Florian and R. Sassot, Phys. Rev. D **69**, 074028 (2004).
[9] K. J. Eskola, V. J. Kolhinen and P. V. Ruuskanen, Nucl. Phys. B **535**, 351 (1998).
[10] K. J. Eskola, V. J. Kolhinen and C. A. Salgado, Eur. Phys. J. C **9**, 61 (1999).
[11] M. L. Mangano, P. Nason, and G. Ridolfi, Nucl. Phys. B **373**, 295 (1992).
[12] M. Cacciari, P. Nason and R. Vogt, Phys. Rev. Lett. **95**, 122001 (2005).